

Modelling, Simulation and Temperature Effect Analysis on Mutual Induction based High Temperature Level Sensor using COMSOL Multiphysics

Rajalakshmi.R¹, Subhasis Dutta², G.J Gorade³, B.S.V.G.Sharma⁴, P.K Vijayan⁵
 1 Instrumentation Section, Reactor Design & Development Group, rajlakshmi@barc.gov.in
 2 Research Reactor Maintenance Division, Reactor Group, sdutta@barc.gov.in
 Bhabha Atomic Research Centre, Mumbai 400 085

Abstract

Mutual Inductance based Level sensor has been proposed for high temperature (1000 °C) molten metal applications. Modelling and Simulation studies are done in FEM software COMSOL 5.1[1] to obtain optimum sensor design, excitation frequency and sensor characteristics. Further temperature effects on the sensor output were studied and compensation techniques [2] were implemented. This paper provides a brief discussion on Conceptual design and Mathematical model [4] of the Sensor, Modelling and simulation studies to obtain the sensor characteristics using COMSOL and experimental validation of COMSOL simulation results.

Keywords- LBE-Lead Bismuth Eutectic, AC/DC module, Heat Transfer module.

1. Introduction

Bhabha Atomic Research Centre (BARC), is currently developing concepts of high temperature reactor capable of supplying process heat of around 1000°C. These Reactors uses liquid metal coolant (LBE) due to its favourable nuclear and excellent heat transfer properties. Level of the liquid metal is an important process parameter which needs to be monitored. The hot and corrosive environment of Lead Bismuth Eutectic alloy inhibits the use of conventional Level measurement techniques commercially available. On the other hand, its high electric conductivity permits to use electromagnetic systems. Thus, a level sensor based on mutual inductance principle been designed and developed for continuous level measurement.

2. Conceptual design and Mathematical model of the Sensor

The sensor works on the principle of variation of mutual inductance between two windings when they are in proximity of a conducting fluid like LBE. The primary winding of the sensor is excited with an AC current source of constant magnitude and frequency as shown in Fig. 1. Due to mutual inductance an EMF is induced in the secondary coil. An EMF is also induced in LBE and eddy current flows in it. The magnetic flux due to eddy current will oppose the main flux produced by the

primary winding. Hence the net flux linked with secondary winding decreases and thereby the secondary voltage reduces with the increase in level of LBE. When the LBE temperature increases, the resistivity of LBE increases, hence the eddy current and the induced voltage is affected. This needs to be compensated to provide output signal independent of LBE temperature.

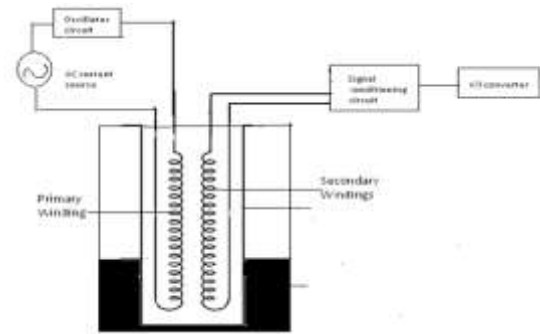


Fig. 1: Sensor Conceptual Design

Since the Primary and Secondary are wound in a bifilar manner they are considered to be fully magnetically coupled. Consider the Primary winding as a solenoid of N number of turns of radius R, the current density through it is \vec{J} . In order to obtain the flux density \vec{B} through the coil, Ampere's law for an Amperian Loop considered along the coil is applied [3, 4]

$$\nabla \times \vec{B} = \mu_0 \vec{J} \quad (1)$$

$$\vec{B} = \mu_0 \mu_r n i \hat{z} \quad (2)$$

Where \hat{z} is the unit vector in the z-direction

In order to obtain the expression of induced voltage v across the primary, Maxwell's equation [3, 4] was solved as below

$$\nabla \times \vec{E} = - \frac{\partial \vec{B}}{\partial t} \quad (3)$$

$$v = \int E dl = - N \frac{\partial \phi}{\partial t} \quad (4)$$

The field outside the coil (in the LBE) is non-zero as for the case of an ideal solenoid, which has a non-zero flux density outside its windings and is given by

$$\vec{B}(r) = \frac{\mu_0 \mu_r i}{2\pi r} \hat{z} \quad (5)$$

The boundary condition used to obtain the expression is

$$\vec{B}(\infty) = 0 \quad (6)$$

$\vec{B}(r)$ Denotes the magnetic flux density with the distance from the center of the primary winding. Consider a layer of liquid metal outside the sensor of thickness dz as shown in Fig. 2 and a circular ring of radius r and thickness dr through the layer, concentric with the cross section of the coil. This forms the assumed path through which eddy current would flow in the liquid metal.

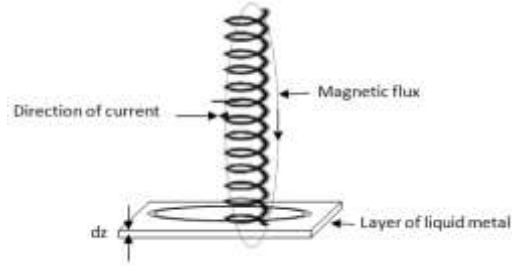


Fig. 2: Electrical Analogy of Sensor in LBE

The conductivity of LBE is given by $\frac{10^8}{(86.334 + 0.0511 \times T)}$ thus is depending on the temperature of the liquid metal [5].

The induced emf in the elemental circular section of the liquid metal is obtained from faraday's law as

$$E_{induced} = \frac{\mu_0 \mu_r r}{2} i_0 \omega \cos \omega t \quad (7)$$

The eddy current flowing through the considered elemental circular path at temperature of 1000K is given by

$$dI = \frac{E_{induced}}{\text{Resistance of the path}} = \frac{\frac{\mu_0 \mu_r r}{2} i_0 \omega \cos \omega t \, dz \, dr}{137.434 \times 10^{-8} \times 2\pi r} \quad (8)$$

$$dI = \frac{\frac{\mu_0 \mu_r}{2} i_0 \omega \cos \omega t \, dz \, dr}{137.434 \times 10^{-8} \times 2\pi}$$

Now, consider the circular current carrying path as a ring carrying current of magnitude given in expression 8. The field at a height of h at the centre of the ring is given by

$$d\vec{B}_z = \frac{\mu_0 \mu_r dI r^2}{2(h^2 + r^2)^{3/2}} = \frac{\mu_0 \mu_r r^2}{2(h^2 + r^2)^{3/2}} \times \frac{\frac{\mu_0 \mu_r}{2} i_0 \omega \cos \omega t \, dz \, dr}{137.434 \times 10^{-8} \times 2\pi} \quad (9)$$

Thus the net flux density along the length of the coil of height H inserted in an enclosure of radius R_E , due to the entire liquid metal of level L in a tank of radius R_T is given by

$$\vec{B}_z = -\mu_0 \mu_r \times \frac{\frac{\mu_0 \mu_r}{2} i_0 \omega}{137.434 \times 10^{-8} \times 16\pi} \times \frac{\cos(\tan^{-1}(\frac{H}{R_T} - 1)) \times \cos(\tan^{-1}(\frac{H}{R_E} + 1))}{\cos(\tan^{-1}(\frac{H}{R_T} + 1)) \times \cos(\tan^{-1}(\frac{H}{R_E} - 1))} \times L \cos \omega t \quad (10)$$

The induced voltage at the secondary due to this flux is given by

$$v_{eddy} = -N \frac{\partial \phi_z}{\partial t} \quad (11)$$

Since the induced voltage at the secondary due to the flux generated by the eddy current in the Liquid metal is in opposition to the voltage due to primary excitation the net effect at the Secondary winding is given by

$$V_0 = |V| - |V_{eddy}| \quad (12)$$

Thus the voltage across the secondary decreases linearly with level of molten LBE.

3. Equations and boundary conditions used in COMSOL

3.1 Equations solved in COMSOL

(a) Heat transfer equations in solids:

$$\rho C_p u \nabla T + \nabla \cdot q = Q$$

$$q = -k \nabla T$$

(b) Ampere's Law:

$$(\nabla \cdot \sigma - \omega^2 \epsilon_0 \epsilon_r) A + \nabla \times (\mu_0 \mu_r)^{-1} B - \sigma \nabla \times B = J$$

(c) Magnetic field density: $B = \nabla \times A$

3.2 Boundary conditions used in COMSOL Simulation

(a) Magnetic Insulation was considered at all boundaries of the geometry. Limiting the values of the magnetic field at the boundaries of the geometry: $n \times A = 0$.

(b) Thermal Insulation was also considered at all boundaries of the geometry: $-n \cdot q = 0$.

(c) The Temperature at the surface of the enclosure is considered to be as the temperature of LBE. The temperature of air at a distance from the tank is considered to be at room temperature. These are being defined to solve heat transport equations.

4. Geometry Modelling of Sensor using COMSOL

Modelling the geometry for the Mutual Inductance based Level sensor was done in 2D axi-symmetric model wizard, owing to the symmetric nature of the geometry involved. The Geometry included MI cables wounded on SS former in a bifilar manner. MI cable used to form the winding of the coil was represented by three concentric circles representing the Copper conductor, the MgO insulator and the SS sheath respectively as shown in Fig. 4. An air gap was modelled between the sensor and SS enclosure containing the sensing probe. The liquid metal surrounding the sensor was represented as shown in Fig. 3. Suitable materials were added in the respective domains in the geometrical Model. In order to obtain the characteristics and calibrate

the sensor for different levels of liquid metal, a parameter was defined to represent the level of LBE and parameter sweep of the same was performed to vary the level of LBE in the tank. Physics Controlled Meshing was used as the sequence type during Meshing. Extremely fine element size was selected for the entire geometry to obtain highly accurate results. Further results were repeated with different mesh sizes. Repeatability of the results was observed.

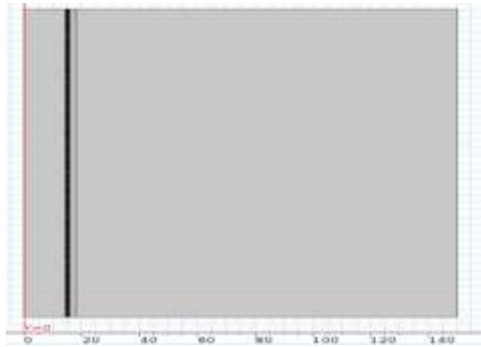


Fig. 3: Geometrical Model of sensor

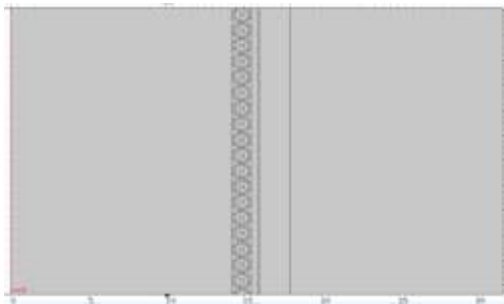


Fig. 4: Bifilar winding on SS former

5. Simulation studies using COMSOL Multiphysics

The multiphysics used for characterization of the level sensor was magnetic field interface in AC/DC module for evaluating the induced voltage at the secondary winding, the effects of liquid metal on the mutual coupling between the two coils of the sensing probe and Heat transfer in fluids interface in Heat Transfer module to study the effects of the change in temperature of LBE in the process of measurement. Temperature coupling was used to evaluate the effect of temperature of LBE on the characteristics of the sensor. Studies were carried out at various frequencies. Stationary domain studies were also carried out in order to obtain the temperature distribution due to the presence of high temperature liquid metal.

To simulate the primary and secondary windings Multi turn coil domain was used in the Magnetic field interface. A Global evaluation was included to evaluate the induced voltage at the secondary coil.

The magnetic flux density distribution around the sensor and the eddy current induced in the molten

metal is as shown in Fig. 5. It can be noted that the magnetic flux density decreases in that portion of the sensor which is under LBE level due to the opposing flux generated by the eddy current induced in LBE. Further the flux density varies between 1.69×10^{-4} T at the centre of the conductor of the Primary winding and decreases to 2.1×10^{-14} T at the bulk of LBE as shown in Fig.6.

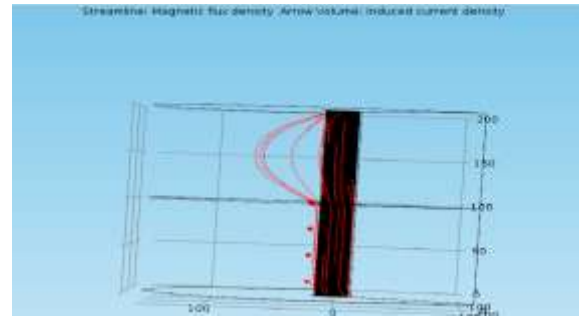


Fig 5: Flux and Eddy current profiles

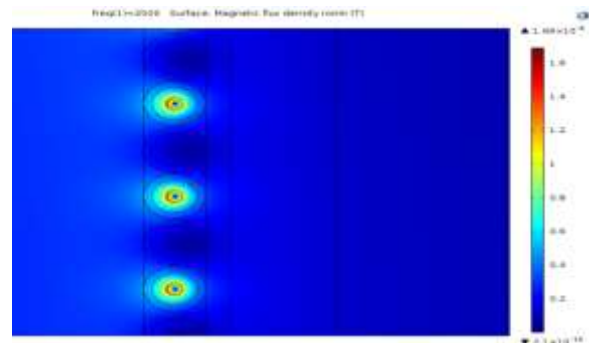


Fig 6: Variation of Flux density

The induced eddy current distribution is shown in Fig.7. The current is maximum at the bulk of the liquid metal. It can be noted that the current induced in the former and the SS enclosure is in opposition to that induced in LBE. The variation in secondary output voltage with level of LBE at different temperatures is shown in Fig. 8. As the primary effect of temperature change on the liquid metal was the change in its conductivity, the same was incorporated in the material properties of LBE. Also the output span of the sensor decreases with the increase in temperature of molten metal.

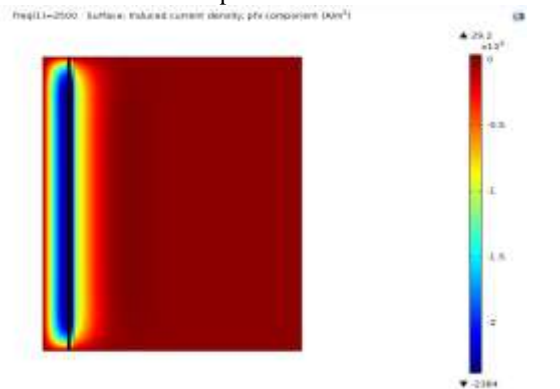


Fig. 7: Variation of Induced eddy current

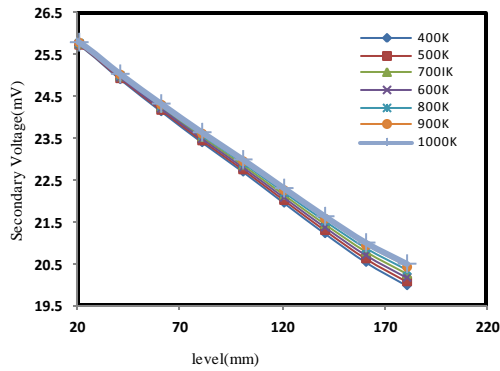


Fig. 8: Secondary Voltage vs. Level at different Temperatures

6. Experimentation

The performance of the sensor was evaluated in an existing setup for a range of 120mm of liquid metal. Further the temperature range of molten metal was limited to 115 °C throughout experimentation

7. Analysis of Simulation results with experimentation

The sensor characteristics obtained from simulation were compared with the results of experimentation. The characteristics of the sensor with different frequency of excitation are shown in fig. 9. It could be noted that the change in output voltage with frequency decreases at higher frequencies. This phenomenon is due to magnetic saturation at higher frequencies of excitation. This was considered as a basis of selecting the optimized frequency as the change in oscillator frequency shall not disturb the sensor output. It is to be noted that higher frequency leads to greater eddy losses in the sensor. Thus optimisation of excitation frequency was done by considering the above mentioned effects. The variations of output from the sensor with the change in level of molten metal obtained from experimentation were compared under similar conditions with that of the COMSOL simulation and are shown in Fig. 10. It can be seen that in both cases the voltage output decreases linearly with Level.

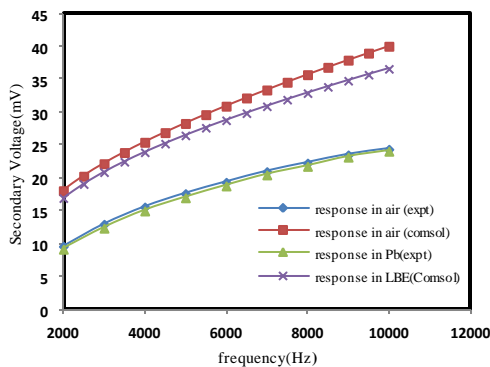


Fig. 9: Variation of Sec. Voltage with frequency

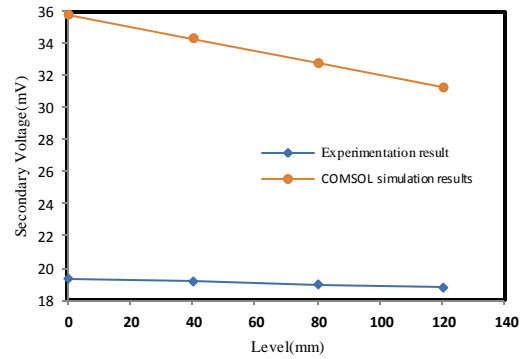


Fig. 10: COMSOL and experimental Results

8. Temperature effect Analysis

The temperature inside sensor enclosure due to various level of LBE was studied at high temperature of 1300K. With the liquid metal at a temperature of 1300K (1027 °C) outside the enclosure, the variation in temperature inside the enclosure with the level of LBE is shown in Fig. 11. The temperature inside the enclosure rises as the liquid level increases in the tank but above 25mm level of LBE the temperature stabilizes to that of the liquid metal outside the enclosure. This has been considered during the computation of resistance of the primary coil with the change in level and Temperature of LBE in the tank.

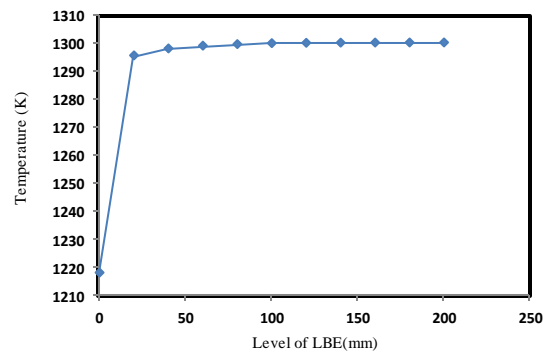


Fig. 11: Variation of probe temperature with level

9. Temperature Compensation

The resistivity of liquid metal changes with its Temperature, this causes a change in the eddy current induced and thus the Secondary emf. Temperature compensation method utilizes an external resistance R_{ext} as discussed in Paris *et al* [2]. The value of the external Resistance is computed with the help of the expression given below

$$R_{ext} = \frac{V_0 \times \partial R_i}{\partial V_0} - R_i \quad (13)$$

R_i is the internal resistance of the secondary winding which is same as the primary, V_0 is secondary output, ∂R_i is difference in internal resistance at extremes of temperatures, ∂V_0 is difference in secondary voltage. Thus the variation

of external resistance for temperature compensation, with the frequency of excitation for the upper and lower range of level of LBE is obtained and shown in Fig. 12. The point of intersection of the plots provides the External Resistance and frequency of excitation which would provide temperature compensation for the given span of level measurement. Further the results were verified experimentally as shown in Fig. 12.

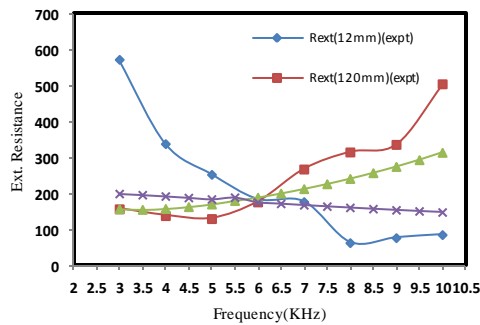


Fig. 12: External Resistance vs. Frequency

Fig. 13 shows the temperature compensated output of the sensor with the variation of LBE level.

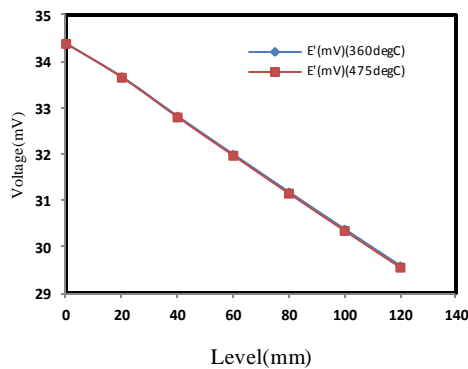


Fig. 13: Voltage a/c external Resistance (COMSOL)

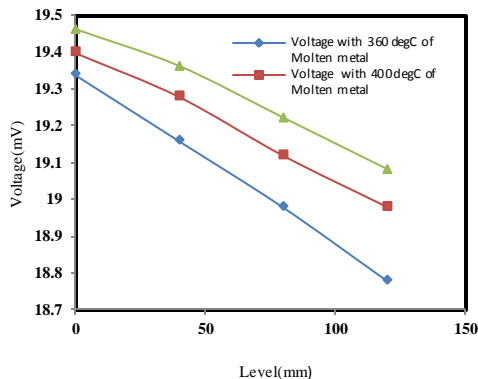


Fig 14: Sec. Voltage vs. Level at different temperatures (Expt)

The variation of Output Voltage due to change in Level of Molten metal at different Temperatures, without temperature compensation, obtained from experimentation is plotted in Fig. 14. The change in voltage with level of liquid metal at different

temperatures measured across the external resistance is also shown in Fig. 15.

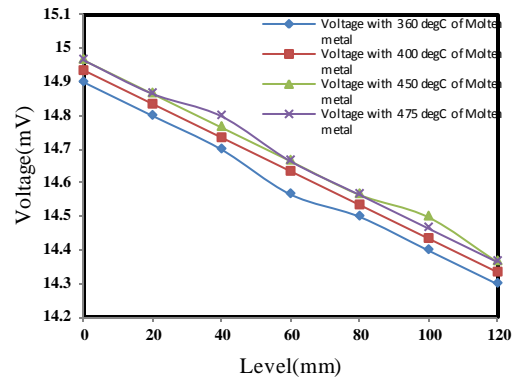


Fig. 15: Voltage a/c ext. Resistance (Expt)

10. Conclusions

The sensor characteristics obtained through COMSOL simulations and experimentation were compared. The Voltage decreases linearly with increase in level of LBE in both the cases. The span experimentally obtained from the sensor for a level range of 0 to 120mm of liquid metal was 0.76 mV, while COMSOL simulations provided a span of 4 mV for the same level variation. The sensor resolution obtained through experimentation was 1.57mm of LBE level, while COMSOL simulations provided a resolution of 0.3mm of LBE level as simulation results showed higher voltage levels for the same range of measurement.

The error due to a 115 °C temperature variation of liquid metal at 100 % level was reduced from 1.1 % of reading to 0.45 % of reading after providing temperature compensation in experimentation. While in COMSOL a reduction in error from 0.21 % of reading to 0.09 % of reading was achieved by temperature compensation.

There is a 43 % difference on an average between the simulation and experimental results. Further this difference reduces with the range of level measurement.

11. References

- [1] COMSOL Reference Manual
- [2] Paris *et al*, Probe for measuring the level of a liquid metal, (1976).
- [3] Uwe Tröltzsch *et al*, Simplified analytical inductance model for a single turn eddy current sensor.
- [4] Prof. Ted Jacobson, Supplement: Phy374, (spring 2006)
- [5] Handbook on Lead-Bismuth Eutectic Alloy and Lead properties, Chapter 2.